CLIMATE CHANGE

The Little Ice Age and 20th-century deep Pacific cooling

G. Gebbie[1]* and P. Huybers[2]

Proxy records show that before the onset of modern anthropogenic warming, globally coherent cooling occurred from the Medieval Warm Period to the Little Ice Age. The long memory of the ocean suggests that these historical surface anomalies are associated with ongoing deep-ocean temperature adjustments. Combining an ocean model with modern and paleoceanographic data leads to a prediction that the deep Pacific is still adjusting to the cooling going into the Little Ice Age, whereas temperature trends in the surface ocean and deep Atlantic reflect modern warming. This prediction is corroborated by temperature changes identified between the HMS Challenger expedition of the 1870s and modern hydrography. The implied heat loss in the deep ocean since 1750 CE offsets one-fourth of the global heat gain in the upper ocean.

Downcore temperature profiles found in boreholes from the Greenland (*1*) and West Antarctic ice sheets (*2*) enable the recovery of past surface temperatures. These borehole inversions indicate a globally coherent pattern of cooling from the Medieval Warm Period to the Little Ice Age that is also documented in recent land (*3*) and ocean (*4*) proxy compilations. The ocean adjusts to surface temperature anomalies over time scales greater than 1000 years in the deep Pacific (*5*, *6*), which suggests that it too hosts signals related to Common Era changes in surface climate (*7*). But whether these signals are predictable or detectable in the face of three-dimensional ocean circulation and mixing processes, let alone invertible for surface characteristics, has been unclear.

To explore how Common Era changes in surface temperature could influence the interior ocean, we first inverted modern-day tracer observations for ocean circulation using a previously described methodology (*8*). In this inversion, the net effects of sub–grid-scale processes on advective and diffusive transport are empirically constrained at a 2° resolution in the horizontal and 33 levels in the vertical. When integrated with prescribed surface values, the estimated circulation gives accurate predictions of interior $\delta^{13}C$ (*9*) and radiocarbon values (*6*). The relative influences of Antarctic Bottom Water and North Atlantic Deep Water are also captured (*8*) and agree with estimates made using related approaches (*10*).

It is also possible to represent the transient oceanic response to changing surface conditions. A 2000-year simulation is performed by initializing our empirical circulation model at equilibrium in 15 CE and prescribing globally coherent surface temperature anomalies (*4*) that propagate into the ocean interior (see supplementary materials). The resulting estimate, referred to as EQ-0015, indicates that disparate modern-day temperature trends are expected at depth (Fig. 1). At depths below 2000 m, the Atlantic warms at an average rate of 0.1°C over the past century, whereas the deep Pacific cools by 0.02°C over the past century.

The pattern of temperature trends can be understood as a basic consequence of an advective-diffusive adjustment to surface conditions. Deep Atlantic waters are directly replenished by their formation in the North Atlantic, but deep Pacific waters must propagate from the Atlantic and Southern oceans. Radiocarbon observations (*11*) indicate that most waters in the deep Atlantic were last at the surface 1 to 4 centuries ago, whereas most deep Pacific waters have longer memory due to isolation from the atmosphere for 8 to 14 centuries (*6*). As a result of differing response times, Atlantic temperature trends reflect warming over recent centuries, including that associated with anthropogenic influences, whereas the Pacific is still cooling as a consequence of ongoing replacement of Medieval Warm Period waters by Little Ice Age waters.

The simulated magnitude of temperature changes also reflects an advective-diffusive response to surface conditions. EQ-0015 indicates deep-Pacific cooling of 0.1°C following the temperature maximum associated with the Medieval Warm Period, whereas the faster-responding deep Atlantic cools by as much as 0.3°C. Ocean circulation can be likened to a filter through which interior water properties inherit a temporally smoothed version of surface signals. Signals in the deep Pacific are more heavily smoothed and have a more attenuated signal than their Atlantic counterparts because they are subject to mixing over a longer journey (*12*). The incomplete response of the subsurface to rapid surface changes also leads to delays seen in EQ-0015 being shorter than those indicated by radiocarbon-age analysis (*13*).

Implicit in the EQ-0015 simulation is that temperature anomalies are transported according to a statistically steady ocean circulation. Estimates of circulation strength over the Common Era, however, suggest variations by as much as ±25% for components of the Atlantic circulation (*14*, *15*). If we instead modify circulation rates to covary with surface temperature anomalies such that advective and diffusive fluxes are changed by ±25% in the Little Ice Age relative to the 1990s, the magnitude of our results is altered (fig. S3), but not the qualitative pattern. In a general circulation model not subject to such simplified assumptions, the centennial-scale subsurface temperature response is also well approximated by the transport of an unchanging circulation (*16*). Of course, it cannot be excluded that changes in deep circulation—for example, in response to altered deep water formation rates or winds (*17*)—counteract the basic pattern of temperature response expected from modern circulation. The results of EQ-0015 are thus considered a prediction that requires further testing.

Differences in the simulated timing and magnitude of temperature trends between the Atlantic and Pacific offer a fingerprint of historical changes in surface temperature. To compare this fingerprint against observations, we turn to the deep-ocean temperature measurements from the HMS Challenger expedition that were obtained near the beginning of the instrumental era, 1872–1876 CE. There were 5010 temperature observations along the cruise track, including 4081 observations below the mixed layer and 760 observations from deeper than 2000 m (Fig. 2). Previous analysis (*18*) showed a 0.4°C warming between the 1870s and 2000s in the upper 500 m of the ocean, tapering off to values indistinguishable from zero at 1800 m depth. Challenger temperature trends were not assessed at deeper levels, however, over concerns regarding depth-dependent biases.

Our focus is to test the model prediction of deep-Pacific cooling. Therefore, we guard against observational biases that would predispose results toward such a trend. In particular, we adjust Challenger temperatures to be 0.04°C cooler per kilometer of depth in keeping with a previously used correction for the effects of compression (*18*, *19*). Another concern is that the rope used for measurements may not have paid out entirely in the vertical, causing depths to be overestimated. But comparing Challenger reports of ocean depth against modern bathymetry (*20*) indicates that, if anything, depths are underestimated, possibly because the hemp rope used aboard the Challenger stretched (fig. S4). We apply no further depth corrections because underestimates would only bias our analysis toward showing greater warming. The exception is in the Southern Ocean, where strong currents are expected to cause greater horizontal deflection of the line (*18*); data south of 45°S are therefore excluded. Finally, the max-min thermometer used on the Challenger would have been biased in regions with vertical temperature inversions. To mitigate the influence of such reversals, we also exclude the 164 data points that are located in temperature inversions in modern climatology (*21*), leaving a total of 3212 observations.

The most recent top-to-bottom global assessment of ocean temperatures comes from the World Ocean Circulation Experiment (WOCE) campaign of the 1990s. Interpolating WOCE

[1]Department of Physical Oceanography, Woods Hole Oceanographic Institution, Woods Hole, MA 02543, USA. [2]Department of Earth and Planetary Sciences, Harvard University, Cambridge, MA 02139, USA.
*Corresponding author. Email: ggebbie@whoi.edu

observations (*21*) to the Challenger data locations permits for comparison of temperatures across more than a century. The squared cross-correlation between WOCE and Challenger temperatures is 0.97 and remains high at 0.92 after removing a global-mean vertical profile from each individual profile. Comparison of other 20th-century hydrographic data also indicated only minor density perturbations on the basic oceanic structure (*22*). Similarity of the oceanic temperature and density structure over time supports the interpretation of changes in circulation since the Little Ice Age as involving only minor perturbations.

Despite overall consistency, there are systematic differences between WOCE and Challenger temperatures. The upper 1000 m of the ocean hosts pervasive warming (Fig. 3), as found earlier (*18*). Basin-wide warming is also found to 2800 m depth in the Atlantic and is significant at the 95% confidence level. Significance levels are computed accounting for the effects of high-frequency motions incurred by internal waves, mesoscale eddies, and wind variability (see supplementary materials). In the deep Pacific, we find basin-wide cooling ranging from 0.02° to 0.08°C at depths between 1600 and 2800 m (Fig. 3) that is also statistically significant. The basic pattern of Atlantic warming and deep-Pacific cooling diagnosed from the observations is consistent with our model results, although the observations indicate stronger cooling trends in the Pacific. Note that the difference between Atlantic and Pacific trends is particularly diagnostic because it is insensitive to choices regarding depth-dependent bias corrections.

The bulk of the Challenger observations that indicate 20th-century cooling are found in the Pacific between 2000 and 4000 m depth. We estimate the integrated rate of heat loss in this Pacific layer to be 1 TW. Although a warming trend was identified in repeat hydrographic observations available over recent decades for the abyssal ocean below 4000 m (*23*), trend estimates specifically for the deep Pacific between 2000 and 4000 m depth were found to be insignificant at 6 ± 7 TW (5 to 95% confidence interval) over the period 1991–2010 (*24*). Reanalysis products augment the hydrographic data with other observational and numerical model information, but no consensus on the sign of deep-Pacific temperature trends has emerged amongst these estimates (*25*). Some reanalyses do, however, show a pattern of Atlantic warming and deep-Pacific cooling that is congruent with our findings (*26*, *27*) (see supplementary materials). Whereas it was suggested that this deep-Pacific cooling in reanalyses originates from model initialization artifacts and weak data constraints (*25*), our results indicate that such temperature drifts should be expected on physical grounds. We also emphasize that there is a major caveat in all these comparisons, in that rate estimates may be sensitive to decadal variability and the time periods over which trends are computed (*7*).

The EQ-0015 simulation is independent of the Challenger observations, and these two indications of deep-ocean temperature trends can be

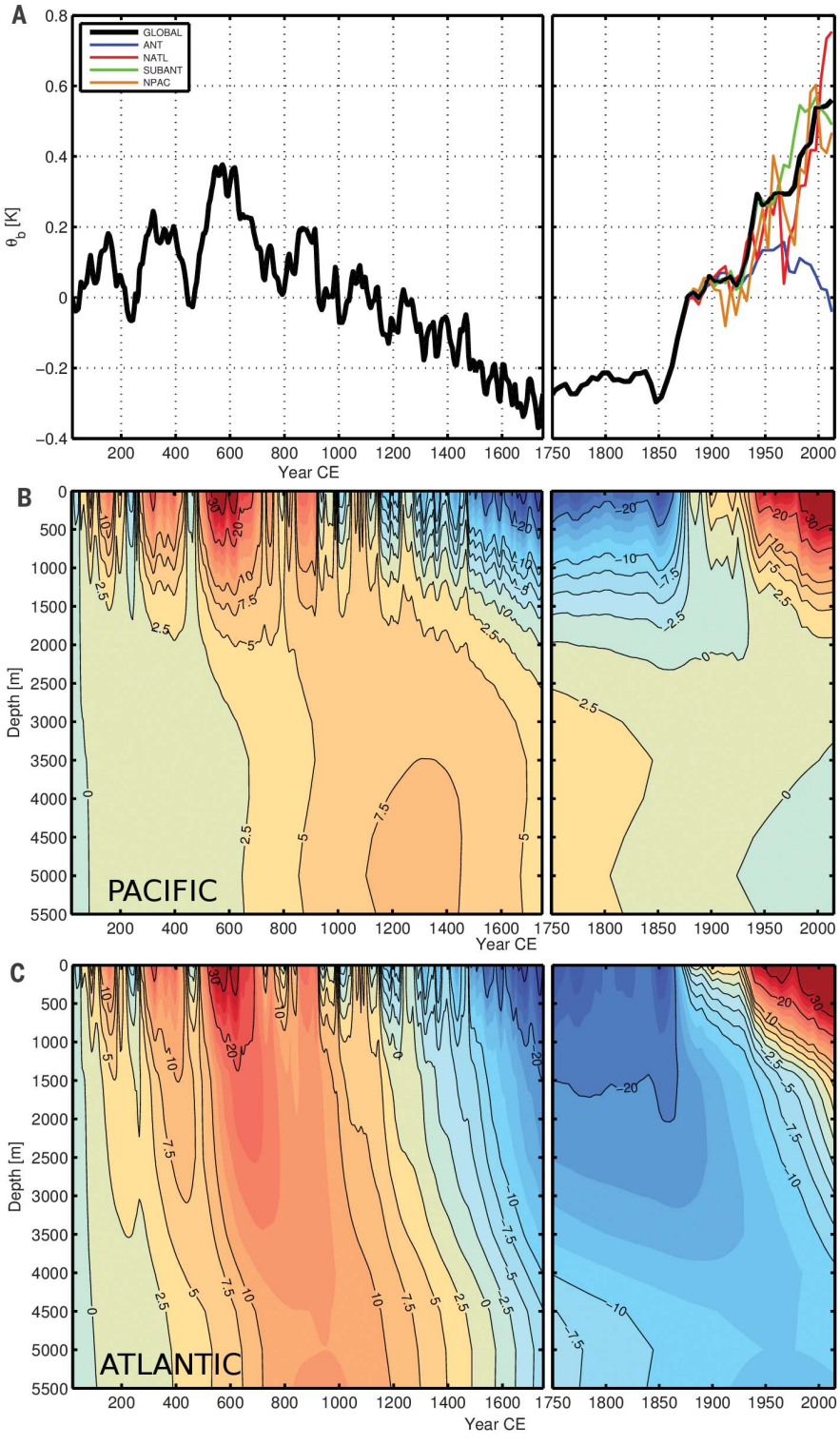

Fig. 1. Simulated interior ocean response to Common Era surface temperature anomalies. (**A**) Global average (black line) and regionally averaged (colored lines) surface temperature time series θ_b, for a simulation initialized from equilibrium in 15 CE (EQ-0015). Regional variations are plotted for the Antarctic (ANT), North Atlantic (NATL), sub-Antarctic (SUBANT), and North Pacific (NPAC). Prior to globally available instrumental surface temperatures beginning in 1870 CE, global changes are prescribed according to estimates from paleoclimate data. (**B**) Time evolution of the Pacific-average potential temperature profile from EQ-0015. (**C**) Similar to (B) but for the Atlantic-average profile. Atlantic and Pacific averages are taken north of 35°S and 45°S, respectively, and color shading has a 2.5-cK interval from −35 to 35 cK. Note the expanded time axis after 1750 CE.

combined to give a more detailed estimate. We first average Challenger-to-WOCE temperature trends over the Atlantic and Pacific basins as a function of depth. These basin-wide average trends are used to relax the assumption of globally uniform changes in surface conditions and to constrain regional temperature histories for 14 distinct regions over the Common Era by a control theory method (see supplementary materials). The result, referred to as OPT-0015, fits the observed vertical structure of Pacific cooling and Atlantic warming (Fig. 3). Global surface changes still explain the basic Atlantic-Pacific difference in OPT-0015, but greater Southern Ocean cooling between 600 and 1600 CE leads to greater rates of cooling in the deep Pacific over recent centuries. Regionally inferred variations in North Atlantic and sub-Antarctic surface temperatures also reproduce an Atlantic warming minimum at 800 m. Because OPT-0015 is constrained using only basin-wide averages, regional temperature patterns can be independently compared against observations. Notable in this regard is that OPT-0015 produces greater rates of cooling in the deep North Pacific and greater warming in the vicinity of the Atlantic deep western boundary current. Similar patterns are evident in the Challenger observations (fig. S7) as well as the average across multiple ocean reanalyses (*25*).

Regional surface temperatures in OPT-0015 can also be compared against ice-core borehole inversions. OPT-0015 places the coldest Antarctic conditions in the 1500s and the coldest North Atlantic in the 1800s, both of which are amplified relative to the global average (Fig. 4). This interhemispheric sequence of peak cooling aligns with the minimum surface temperatures estimated from boreholes in Antarctica (*2*) and Greenland (*1*). A second, weaker cool interval inferred from Greenland boreholes between 1400 and 1600 CE (*1*) is, however, not found for the North Atlantic in OPT-0015. The inference of amplified temperature anomalies in the Antarctic and North Atlantic oceans is also consistent with stronger positive feedbacks at high latitudes. Amplification of high-latitude signals could also stem from greater winter than summer cooling during the Little Ice Age (*28*) and from the greater sensitivity of deep-water formation to winter conditions (*29*). The combination of greater volatility in winter surface conditions and greater sensitivity of interior waters to these conditions may explain observations of amplified mid-depth temperature variability relative to the surface over the Holocene (*30*, *31*).

The OPT-0015 results provide an estimate of full-ocean changes in heat content over the Common Era. With regard to changes in heat content in the upper 700 m of the ocean (Fig. 4), there is excellent consistency between OPT-0015 and results from observational analyses (*32*) and model simulations (*33*), each indicating ~170 ZJ (1 ZJ = 10^{21} J) of heat uptake between 1970 and 2010 (Fig. 4). Over a longer period, 1875–2005, OPT-0015 gives 330 ZJ of global upper-ocean heat uptake, equal to the central estimate from an earlier analysis of upper-ocean heating using

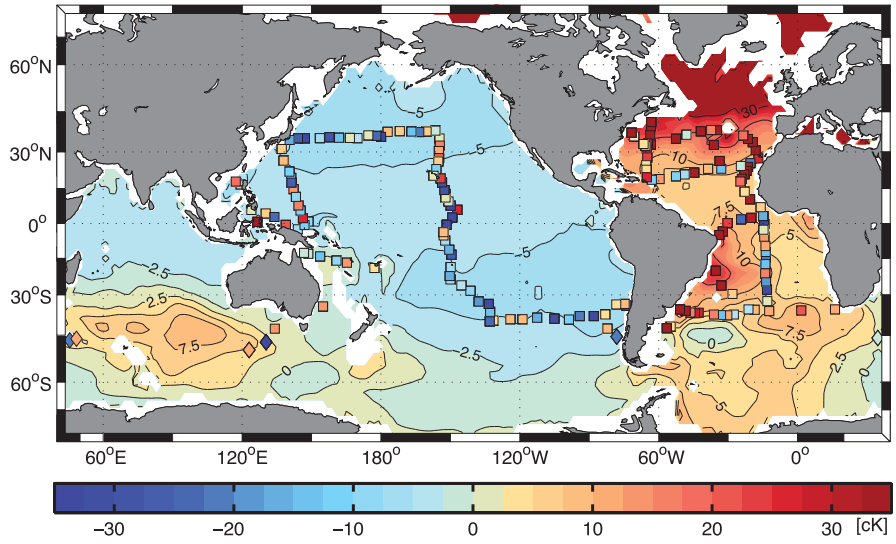

Fig. 2. Observed and simulated deep-ocean temperature changes. Observed ocean temperature changes are diagnosed by differencing WOCE and Challenger temperature measurements. WOCE temperatures are linearly interpolated to the location of Challenger temperatures, and differences are plotted after averaging between 1800 and 2600 m depth (colored markers). Simulated temperature changes for the same depth interval are diagnosed from OPT-0015. Color scaling is equivalent for observed and simulated temperature changes.

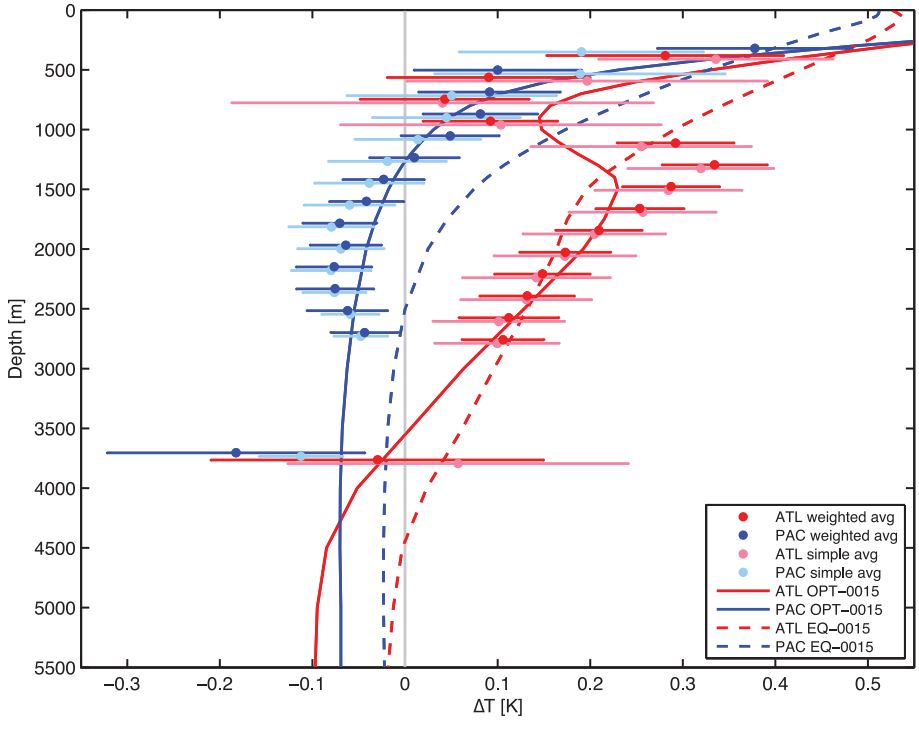

Fig. 3. Vertical profiles of temperature change. Difference between WOCE and Challenger temperatures is shown as a function of depth with 95% confidence intervals averaged over the Pacific (blue) and Atlantic (red). Features of the WOCE-Challenger temperature difference are reproduced in a simulation initialized from equilibrium at 15 CE (EQ-0015, dashed curves) and an inversion constrained by the observations (OPT-0015, solid curves). WOCE-Challenger temperature differences are calculated using a weighted average that accounts for the covariance of ocean temperatures and their uncertainties based on the expected effects of high-frequency oceanic variability (markers and error bars with darker colors). For comparison, a simple average for each basin and depth level is also shown with uncertainties that are empirically estimated (lighter colors).

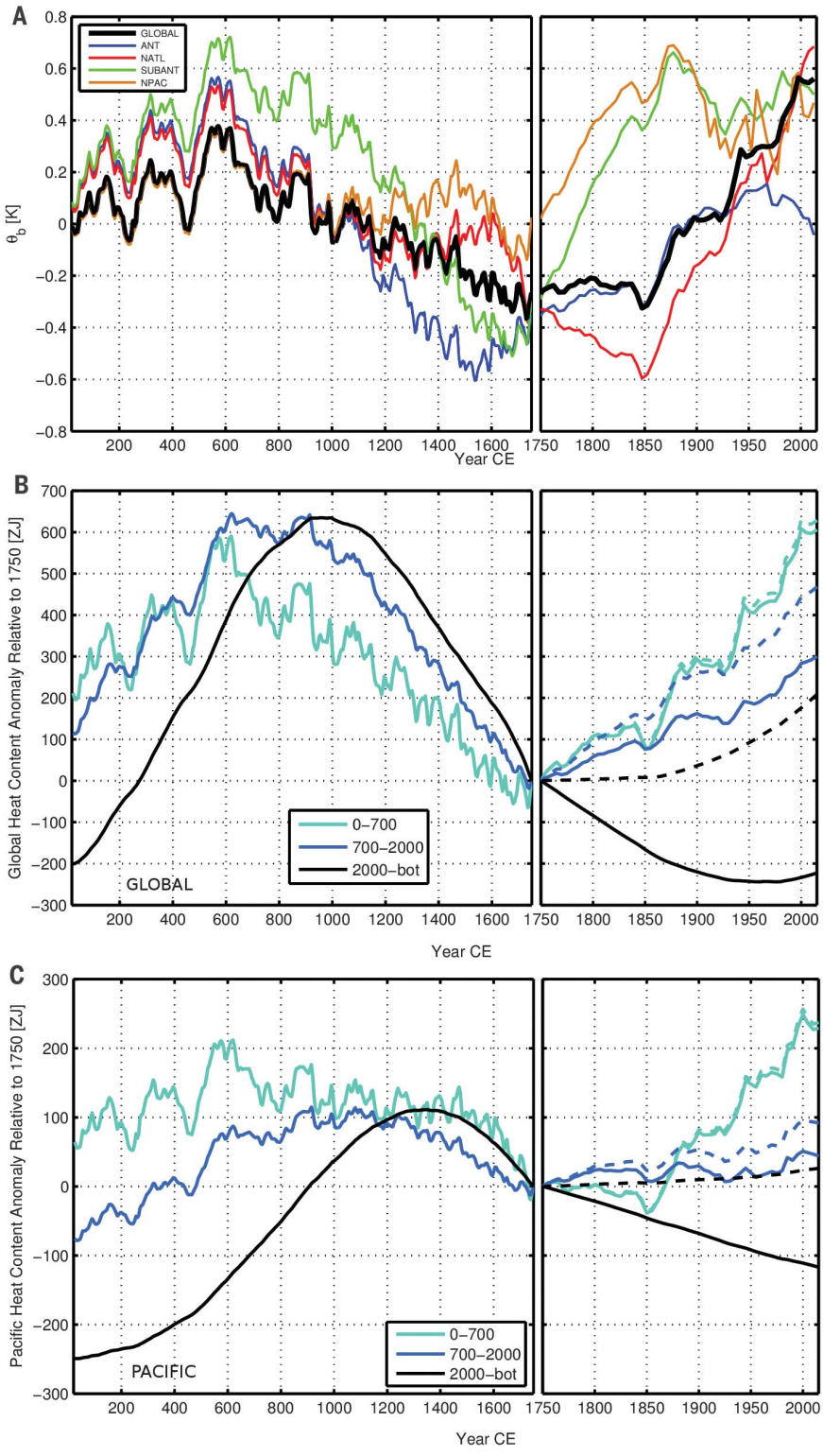

Fig. 4. Regional surface temperature variations and changes in ocean heat content over the Common Era. (**A**) Surface temperature time series after adjustment to fit the HMS Challenger observations (OPT-0015), including four major surface regions (colored lines) and the global area-weighted average (black line). (**B**) Time series of global oceanic heat content anomalies relative to 1750 CE from OPT-0015 as decomposed into upper (cyan, 0 to 700 m), mid-depth (blue, 700 to 2000 m), and deep (black, 2000 m to the bottom) layers. Heat content anomalies calculated from an equilibrium simulation initialized at 1750 (EQ-1750, dashed lines) diverge from the OPT-0015 solution in deeper layers. (**C**) Similar to (B) but for the Pacific. Heat content anomaly is in units of zettajoules (1 ZJ = 10^{21} J).

Challenger observations (*18*). More generally, OPT-0015 indicates that the upper 2000 m of the ocean has been gaining heat since the 1700s, but that one-fourth of this heat uptake was mined from the deeper ocean. This upper-lower distinction is most pronounced in the Pacific since 1750, where cooling below 2000 m offsets more than one-third of the heat gain above 2000 m.

The implications of the deep Pacific being in disequilibrium become more apparent when compared to a counterfactual scenario where the ocean is fully equilibrated with surface conditions in 1750 CE. That the deep Pacific gains heat in this scenario, referred to as EQ-1750, confirms that heat loss in OPT-0015 results from the cooling associated with entry into the Little Ice Age. Moreover, the EQ-1750 scenario leads to 85% greater global ocean heat uptake since 1750 because of excess warming below 700 m. It follows that historical model simulations are biased toward overestimating ocean heat uptake when initialized at equilibrium during the Little Ice Age, although additional biases are also likely to be present (*34*). Finally, we note that OPT-0015 indicates that ocean heat content was larger during the Medieval Warm Period than at present, not because surface temperature was greater, but because the deep ocean had a longer time to adjust to surface anomalies. Over multicentennial time scales, changes in upper and deep ocean heat content have similar ranges, underscoring how the deep ocean ultimately plays a leading role in the planetary heat budget.

REFERENCES AND NOTES

1. D. Dahl-Jensen *et al.*, *Science* **282**, 268–271 (1998).
2. A. J. Orsi, B. D. Cornuelle, J. P. Severinghaus, *Geophys. Res. Lett.* **39**, L09710 (2012).
3. PAGES 2k Consortium, *Nat. Geosci.* **6**, 339–346 (2013).
4. H. V. McGregor *et al.*, *Nat. Geosci.* **8**, 671–677 (2015).
5. F. Primeau, *J. Phys. Oceanogr.* **35**, 545–564 (2005).
6. G. Gebbie, P. Huybers, *J. Phys. Oceanogr.* **42**, 291–305 (2012).
7. C. Wunsch, P. Heimbach, *J. Phys. Oceanogr.* **44**, 2013–2030 (2014).
8. G. Gebbie, P. Huybers, *J. Phys. Oceanogr.* **40**, 1710–1728 (2010).
9. G. Gebbie, P. Huybers, *Geophys. Res. Lett.* **38**, L06604 (2011).
10. T. DeVries, F. Primeau, *J. Phys. Oceanogr.* **41**, 2381–2401 (2011).
11. R. M. Key *et al.*, *Global Biogeochem. Cycles* **18**, GB4031 (2004).
12. M. Holzer, F. Primeau, *J. Geophys. Res.* **115**, C12021 (2010).
13. É. Delhez, É. Deleersnijder, *Cont. Shelf Res.* **28**, 1057–1067 (2008).
14. D. C. Lund, J. Lynch-Stieglitz, W. B. Curry, *Nature* **444**, 601–604 (2006).
15. S. Rahmstorf *et al.*, *Nat. Clim. Chang.* **5**, 475–480 (2015).
16. J. Marshall *et al.*, *Clim. Dyn.* **44**, 2287–2299 (2015).
17. M. Kawase, *J. Phys. Oceanogr.* **17**, 2294–2317 (1987).
18. D. Roemmich, W. J. Gould, J. Gilson, *Nat. Clim. Chang.* **2**, 425–428 (2012).
19. P. Tait, *On the Pressure-Errors of the "Challenger" Thermometers*, Narrative of the Challenger Expedition, Vol. II, Appendix A (HM Stationery Office, 1882).
20. British Oceanographic Data Centre, *GEBCO Digital Atlas* (2003); www.bodc.ac.uk/projects/data_management/international/gebco/gebco_digital_atlas.
21. V. Gouretski, K. Koltermann, *WOCE Global Hydrographic Climatology* (Tech. Rep. 35, Berichte des Bundesamtes für Seeschifffahrt und Hydrographie, 2004).
22. D. Roemmich, C. Wunsch, *Nature* **307**, 447–450 (1984).

23. S. G. Purkey, G. C. Johnson, *J. Clim.* **23**, 6336–6351 (2010).
24. D. G. Desbruyères, S. G. Purkey, E. L. McDonagh, G. C. Johnson, B. A. King, *Geophys. Res. Lett.* **43**, 10356–10365 (2016).
25. M. Palmer *et al.*, *Clim. Dyn.* **49**, 909–930 (2017).
26. I. Fukumori, *Mon. Weather Rev.* **130**, 1370–1383 (2002).
27. A. Köhl, *Q. J. R. Meteorol. Soc.* **141**, 166–181 (2015).
28. A. Atwood, E. Wu, D. Frierson, D. Battisti, J. Sachs, *J. Clim.* **29**, 1161–1178 (2016).
29. H. Stommel, *Proc. Natl. Acad. Sci. U.S.A.* **76**, 3051–3055 (1979).
30. Y. Rosenthal, B. K. Linsley, D. W. Oppo, *Science* **342**, 617–621 (2013).
31. Y. Rosenthal, J. Kalansky, A. Morley, B. Linsley, *Quat. Sci. Rev.* **155**, 1–12 (2017).
32. S. Levitus *et al.*, *Geophys. Res. Lett.* **39**, L10603 (2012).
33. P. J. Durack, P. J. Gleckler, F. W. Landerer, K. E. Taylor, *Nat. Clim. Chang.* **4**, 999–1005 (2014).
34. J. M. Gregory *et al.*, *Geophys. Res. Lett.* **40**, 1600–1604 (2013).

ACKNOWLEDGMENTS

We thank C. Wunsch for highlighting the potential influence of past climate events in the modern ocean; D. Halpern for pointing us to the HMS Challenger data; U. Ninnemann, K. Nisancioglu, T. Eldevik, T. Furevik, Y. Rosenthal, D. Roemmich, L. H. Smedsrud, and T. Stocker for discussions; and three anonymous reviewers for suggestions. **Funding:** Supported by the James E. and Barbara V. Moltz Fellowship and NSF grant OCE-1357121 (G.G.) and by NSF grant OCE-1558939 (P.H.). **Author contributions:** G.G. and P.H. performed the research and the writing. G.G. contributed as lead author; P.H. contributed as the co-author.

Competing interests: The authors declare that they have no competing financial interests. **Data and materials availability:** Data to reproduce the findings are available at the National Centers for Environmental Information, accession number 0178641.

SUPPLEMENTARY MATERIALS

www.sciencemag.org/content/363/6422/70/suppl/DC1
Materials and Methods
Supplementary Text
Table S1
Figs. S1 to S9
Movie S1
References (*35*–*46*)

15 September 2018; accepted 12 November 2018
10.1126/science.aar8413

Science

The Little Ice Age and 20th-century deep Pacific cooling

G. Gebbie and P. Huybers

Science **363** (6422), 70-74.
DOI: 10.1126/science.aar8413

Deep Pacific cooling

Earth's climate cooled considerably across the transition from the Medieval Warm Period to the Little Ice Age about 700 years ago. Theoretically, owing to how the ocean circulates, this cooling should be recorded in Pacific deep-ocean temperatures, where water that was on the surface then is found today. Gebbie and Huybers used an ocean circulation model and observations from both the end of the 19th century and the end of the 20th century to detect and quantify this trend. The ongoing deep Pacific is cooling, which revises Earth's overall heat budget since 1750 downward by 35%.

Science, this issue p. 70